SSrv manuscript No.
(will be inserted by the editor)

Time-variability in the Interstellar Boundary Conditions of the Heliosphere over the past 60,000 years:

Impact of the Solar Journey on the Galactic Cosmic Ray Flux at Earth

Priscilla C. Frisch · Hans-Reinhard Mueller

Received: date / Accepted: date

Abstract During the solar journey through galactic space, variations in the physical properties of the surrounding interstellar material (ISM) modify the heliosphere and modulate the flux of galactic cosmic rays (GCR) at the surface of the Earth, with consequences for the cosmogenic radionuclides at Earth. The diverse ram pressures and ionization levels of ISM possible in the low density solar environment generate dramatically different possible heliosphere configurations, with a wide range of particle fluxes of interstellar neutrals and their secondary products, as well as GCR arriving at Earth. However, simple models of the distribution and densities of ISM in the downwind direction give cloud transition timescales that can be directly compared with cosmogenic radionuclide geologic records. Both the interstellar data and cosmogenic radionuclide data are consistent with cloud transitions within the past 10,000 years and 20,000–30,000 years ago, although the many assumptions about the ISM that are made in arriving at these numbers indicate that the uncertainties are quite large.

Keywords ISM · Heliosphere · Cosmogenic radionuclides

1 Introduction

The Sun has traversed multiple interstellar clouds during our 220 Myr journey around the galactic center, including dense clouds, low density partially ionized interstellar matter (ISM) such as now surrounds the heliosphere, and hot very tenuous plasma. Variations in the galactic cosmic fluxes at the surface of the Earth are strongly dependent on the solar activity cycle, the geomagnetic field, and the physical properties of the circumheliospheric interstellar material. The modulation of the 1 AU galactic cosmic ray flux by solar flare mass ejections has long been known (Gosling 1964). The sensitivity of the heliosphere configuration to the total interstellar pressure, including

Priscilla C. Frisch
University of Chicago, Chicago, IL
E-mail: frisch@oddjob.uchicago.edu

Hans-Reinhard Mueller
Dartmouth College, Hanover, NH
E-mail: hans.mueller@dartmouth.edu

the dynamic ram pressure and magnetic pressure (Holzer 1989) indicate that the global heliosphere is a weather vane for the circumheliospheric ISM (CISM). Sufficient data on interstellar absorption lines are now available that the general characteristics of the circumheliosphere ISM can be reconstructed for the past $\sim 100,000$ years (Section 2), providing a basis for evaluating the ISM-modified heliosphere (Section 3), and comparing these historical variations with the geologic radio-isotope record (Section 4). Any scenario connecting features in the geomagnetic record with interstellar cloud encounters will necessarily include assumptions about the ISM, as well as an incomplete understanding of galactic cosmic ray (GCR) modulation for variable heliosphere configurations. Our conclusions below linking cloud transitions to discontinuities in the geologic radioisotope record are subject to these uncertainties.

2 Contemporary and Paleointerstellar CISM

2.1 Dynamics, Structure, and Interstellar Magnetic Field in contemporary ISM

The local solar environment has been sculpted by stellar winds and supernovae originating in stellar associations bordering the Local Bubble (Frisch *et al.* 2009, F09). Fig. 1 shows the Local Bubble cavity, the S1 and S2 shells, and the local standard of rest (LSR [1]) motions of the Sun and CLIC through the cavity. The global ISM has local consequences, since stars in the Local Bubble cavity create local ionization gradients. The cluster of local interstellar clouds (CLIC) flows through the Local Bubble cavity, and provides the contemporary CISM and paleoCISM. The Sun has recently emerged from very low density interstellar gas, < 0.005 cm^{-3} (based on density limits set by the soft X-ray background, F09), and entered the CLIC. This follows from the solar velocity through the local inertial frame (LSR), $V_{\rm sun}= 18.0 \pm 0.9$ km s^{-1}, towards ℓ, $b= 47.9^\circ \pm 3.0^\circ$, $23.8^\circ \pm 2.0^\circ$, the configuration of the CLIC, and from the CLIC LSR velocity of –16.8 km s^{-1} arriving from the direction $\ell\sim 335^\circ$, $b\sim -7^\circ$ (Frisch and Slavin 2006). The CLIC LSR upwind direction coincides with the center of the Loop I (North Polar Spur) supernova remnant centered near ℓ,b=320°,5° in the Sco-Cen Association (Heiles 1998).

The CLIC is a decelerating flow of ISM. ISM kinematics towards nearby stars show the galactic environment of the Sun changes rapidly. From upwind to downwind, interstellar velocities in the solar inertial system ("heliocentric", HC) are –28.4 km s^{-1} towards 36 Oph, 26.3 km s^{-1} in the inner heliosphere, and 23.4 km s^{-1} towards χ^1 Ori. If all other cloud parameters are the same, there is a 50% difference in the ram pressures of these clouds, which alone leads to a significant distortion of the heliosphere. Using $V_{\rm HC}$ for nearby clouds in Table 1, variations in the interstellar ram pressure on the heliosphere may be a factor of 4.2 over the past 10^5 years. If all local clouds have the same density as the CISM, n(H°)=0.2 cm^{-3}, then $\sim 35\%$ of sightlines to stars within 10 pc are filled with warm low density ISM. The clouds have a mean length 0.9 ± 0.3 pc, and the Sun would cross these clouds with a mean crossing time of $\sim 47,000$ years. In the upwind direction, 60% of space towards α Aql contains ISM, while 29% of the space downwind towards α CMa is filled. The heliospheric boundary conditions are set by the CISM, which flows through the heliosphere at ~ 26 km s^{-1} and is replenished every ~ 25 years.

[1] The local standard motion, LSR, is derived from the UVW components in (Schönrich *et al.* 2010, SBD10). LSR velocities here are quoted based on this value for the solar apex motion.

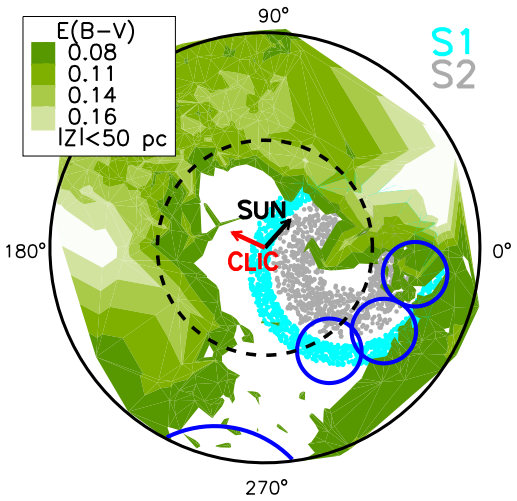

Fig. 1 The distribution of ISM, marked by color excess E(B-V) towards nearby stars. A projected slice along the galactic plane is shown, centered on the Sun, radius 200 pc, perpendicular extent Z= 0±50 pc. The visual extinction towards a star is $\sim 3{\times}E(B-V)$, so that $E(B-V)$ represents the cumulative amount of ISM. The features dominating the past and future solar galactic environment include the distribution of ISM, the LSR vector motions of the CLIC (red arrow) and the Sun (black arrow), and the distribution of hot nearby stars. The local interstellar magnetic field (ISMF) direction is directed towards ℓ,b= 38°, 23°, with uncertainties of ±35°, and overlaps the solar motion in this projection. The Sun is most likely embedded in the S1 magnetic subshell of Loop I that has expanded to the solar location, while the S1 shell tangent line at the Sun (according to the spherical symmetry modeled by Wolleben (2007)) is nearly perpendicular to the CLIC LSR vector flow. $E(B-V)$ contour levels of 0.08, 0.11, 0.14, 0.16 mag correspond to N(H°+H_2) column densities of 4.46e20, 6.56e20, 7.87e20, and 9.18e20 cm^{-2}, for N(H°+H_2)/$E(B-V)$= 5.8×10^{21} atoms cm^{-2} mag (Bohlin *et al.* (1978)). The large blue circles show the three subgroups of the Sco-Cen Association, and the arc centered near $\ell\sim$ 260° shows the approximate nearside of the Gum Nebula. The intersection of the S1 and S2 magnetic shells with the galactic plane are shown as the small cyan-blue and gray dots, respectively.

The heliosphere boundary conditions are determined from self-consistent modeling of the ionization gradients in the CISM, using as constraints data on interstellar He° and pickup ions in the heliosphere, and very local ISM towards ϵ CMa (Slavin and Frisch 2008, S08). The interstellar radiation field is the sum of diffuse ultraviolet radiation dominated by ϵ CMa, the soft X-ray background, extreme ultraviolet emission from a conductive boundary on the local interstellar cloud that ionizes He°, and the radiation flux for $\lambda > 912$ A that regulates the equilibrium of ISM diagnostics such as Mg° / Mg$^+$ ratio and Ca$^+$. A good fit to the LIC data towards ϵ CMa is found for n(H°)=0.19 cm^{-3}, $n_{\rm e}$=0.065 cm^{-3}, $n_{\rm p}$=0.055 cm^{-3}, and T=6,300 K (Model 26 in SF08). The fractional ionizations of H and He are respectively, 22% and 39%. Even in the absence of hot plasma filling the Local Bubble interior, as suggested by modeling of foreground X-rays from charge exchange between the solar wind and interstellar neutrals (Koutroumpa *et al.* 2009), the SF08 models predict a low density, warm partially ionized CISM (Model 42 in SF08). The gas-phase abundances in the

CISM, which include unobserved H^+, provided the first evidence that the Sun is in shocked ISM. The abundance pattern in the gas is characteristic of the destruction of refractory grains in 50–100 km s^{-1} shock fronts, such as associated with expanding superbubble shells (Frisch *et al.* 1999). Abundances of the refractory elements Mg, Si, and Fe are below solar by factors of 3–15, and C is overabundant. However these abundances are larger by factors of 4–8 than cold cloud gas-phase abundances, where grains are quiescent.

The direction of the interstellar magnetic field near the Sun is approximately perpendicular to the CLIC LSR velocity. The best-fitting ISMF direction has been estimated from fits to polarized starlight, caused by attenuation of magnetically aligned interstellar dust grains towards stars within 40 pc. The local ISMF direction is towards $\ell, b = 38^\circ, 23^\circ$, with uncertainties of $\sim \pm 35^\circ$ (Frisch *et al.* 2010). Forming an angle of $\sim 70^\circ$ with the LSR bulk flow CLIC vector, this direction suggests an ISMF compressed in an expanding superbubble shell. The S1 subshell of the Loop I superbubble has a local configuration that is perpendicular to the bulk flow of the CLIC through the LSR, and that is approximately parallel to the ISMF direction (Fig. 1). The ISMF direction indicated by the Interstellar Boundary Explorer (IBEX) Ribbon arc center, ℓ,b= $33^\circ, 55^\circ$ (Frisch and McComas 2010, this volume) agrees with the polarization direction to within uncertainties. Fits to the Faraday rotation and dispersion measures for four pulsars, 150–300 pc away in the third galactic quadrant, give an ISMF direction that is consistent with the polarization data and a field strength ~ 3.3 μG (Salvati 2010).

Some notion of the local ISM configuration is needed to estimate temporal changes in the heliosphere boundary conditions. Data on neutral and electron volume densities of nearby clouds are sparse, so simplifications are unavoidable. For a cloud density of $n(H^\circ) \sim 0.2$ cm^{-3}, the LIC towards Sirius has a thickness of 0.65 pc (Table 1). The angular extent of the LIC is $\sim 150^\circ$ (Redfield and Linsky 2008). If the LIC is 1.0 pc away, it has a length of 7.5 pc, and aspect ratio of 12:1, which is a filamentary structure. For the G-cloud, the angular extent is about 170°, and the cloud thickness towards 36 Oph is 1.15 pc. This gives a cloud length of 22.9 pc, for a distance of 1.0 pc and density 0.2 cm^{-3}, for an aspect ratio of 20:1. The nearest parts of the CLIC therefore seem to be filamentary. A filamentary structure for local clouds is consistent with the polarization evidence linking the flow of ISM past the Sun to an evolved magnetic superbubble shell.

Not all nearby clouds are warm and diffuse. Tiny scale atomic structures (TSAS) are observed throughout the ISM, with typical sizes 30 AU, volume densities $\sim 10^3$ cm^{-3}, column densities $10^{18}-10^{19}$ cm^{-2}, and thermal pressures $P/k = nT = 10^4-10^6$ cm^{-3}K if clouds are spherical (Stanimirović 2009). Towards the constellation of Leo and within 12 pc, a tiny dense cold filamentary interstellar cloud, thickness < 0.4 pc, has been identified in Na° absorption (Meyer *et al.* 2006). TSAS are associated with warm tenuous ISM, and may form in converging interstellar flows. The Leo cloud occurs where the S1 and S2 shells may collide (Frisch 2010). Alternate types of nearby ISM include conductive boundaries between warm diffuse gas and hot plasma between the clouds. Unsaturated outflows of ISM from the clouds lead to sharp gradients in the ISM density, velocity, and temperature over small spatial scales. The outflow velocity can be up to 20 km s^{-1}, with temperature variations of an order of magnitude, over distances < 0.5 pc (SF08).

2.2 Historical changes in the Circumheliospheric ISM over $\sim 100,000$ years

Inferring historical variations in the heliosphere due to the Sun's trajectory through a dynamic inhomogeneous medium requires some basic assumptions about cloud shape and homogeneity. Useful data include H° or D° column densities and velocities. When several sightlines probe a single cloud, the 3D cloud velocity vector is recovered through fits to the velocity components sampling the cloud. The local clouds identified by Redfield and Linsky (2008, RL08) present the most complete velocity structure for the CLIC, but yield a result that the CISM as identified by interstellar He° inside of the heliosphere is not seen towards any other star.

Data on several interstellar clouds identified within 5 pc of the Sun are assembled in Table 1, which also gives simple estimates of cloud crossing times and cloud thicknesses for the assumption that all clouds have the same density as the CISM, or $n(\mathrm{H}^\circ) \sim 0.2$ cm^{-3}. Cloud thickness is $\delta \sim N(\mathrm{H}^\circ)/n(\mathrm{H}^\circ)$, and the crossing time T is $T = \delta/\mathrm{V_{HC}}$. There is a 5% uncertainty in T because of differences in measurements of the cloud velocity. Uncertainties from the assumption of constant H° density are not known, but could be factors of two. We now estimate the timeline for past solar traversals of clouds using the data in Table 1 and assuming (1) the cloud surface is flat and perpendicular to the sightline so that $T = \delta/V_{\mathrm{HC}}$ is valid (see above), or alternatively (2) the cloud is a filamentary structure and roughly aligned with the local ISMF.

The direction towards χ^1 Ori, 9 pc, looks through the heliosphere tail ($\phi_{\mathrm{HeI}} = 13^\circ$) so for a smooth cloud shape the simple estimate should approximate the entry time of the Sun into CISM gas, giving $\sim 60,500$ years ago. For the more distant star in the downwind direction α Aur, which is also close to the tail direction ($\phi_{\mathrm{HeI}} = 28^\circ$) but with higher H° column densities, the Sun entered the ISM 126,000 years ago. Both

Table 1 Crossing times for Clouds Close to Sun [(1)]

Star	ℓ, b, Dist (deg,deg, pc)	V_{HC}, V_{LSR} km s^{-1}	log $N(\mathrm{H}^\circ)$ cm^{-2}	δ, Cloud Thickness (pc)	$\theta_{\mathrm{CLIC}}, \phi_{\mathrm{HeI}}$ LSR, HC (deg)	T, Crossing Time (years)
α Cen	316, -1, 1.3	-18.0, -18.6	17.61	0.66	20°, 130°	(35,900)
α CMa	227, -9, 2.7	19.6, 2.2	17.60	0.65	106°, 42°	32,200
α CMa	227, -9, 2.7	13.7, -3.7	17.40	0.41	106°, 42°	29,000
α CMi	214, 13, 3.5	24.0, 10.4	17.81	1.86	122°, 41°	42,600
α CMi	214, 13, 3.5	20.5, 6.5	18.08	1.38	122°, 41°	92,900
χ^1 Ori	188, -3, 9	22.3, 27.4	17.93	1.38	146°, 13°	60,500
α Aur	163, 4, 13	21.8, 15.3	18.24	2.82	171°, 28°	126,000
36 Oph	358, 7, 6	-28.2, -16.7	17.85	1.15	26°, 170°	(39,800)
ϵ CMa	240.,-11.,133.	17, -0.2	17.60	0.65	86°, 54.°	37,000
ϵ CMa	240.,-11.,133.	10, -7.2	17.48	0.49	86°, 54.°	47,900

[(1)] Columns 1 and 2 are, respectively, the star name, galactic coordinates, and distance. Column 3 gives the velocities of the interstellar absorption components in the solar (e.g., Redfield and Linsky (2008)) and LSR inertial systems. Column 4 is the cloud column density, from Wood *et al.* (2005) or Hebrard *et al.* (1999). Column 5 is the cloud thickness, $N(\mathrm{H}^\circ)/n(\mathrm{H}^\circ)$ calculated for volume density $n(\mathrm{H}^\circ) = 0.2$ cm^{-3}. The angles θ_{CLIC} and ϕ_{HeI} are, respectively, the angles between the star and the LSR upwind CLIC direction (ℓ, $b = 335^\circ, -7^\circ$), and the heliocentric (HC) downwind He° vector (ℓ, $b = 184^\circ, -15^\circ$), respectively. Column 7 gives a nominal crossing time for the cloud, calculated from the cloud thickness and V_{HC}.

clouds are at the LIC velocity. For a continuous ISM distribution, the LIC extends beyond χ^1 Ori and the Sun entered the complex $\sim 126,000$ years ago. However, since the average spatial densities in the two sightlines differ by a factor of 1.5, the option that the LIC velocity component represents two clouds with different properties but the same velocity seems likely, so these two sightlines suggest two cloud transitions. The most recent transition was within the past $\sim 60,500$ years for χ^1 Ori. The earlier transition was before $\sim 400,000$ years ago for the ISM beyond χ^1 Ori, and in front of α Aur, since the cloud moves ~ 22 parsecs per Myrs with respect to the Sun according to the velocity. The sightline towards α CMi, 3.5 pc, is oblique to the He° downwind vector ($\phi_{\rm HeI}$=41°), but appears to have absorption at the two velocities of the LIC and Blue Cloud (BC) seen towards α CMa. This sightline gives an entry time into the LIC less than 92,900 years ago. The absence of a distinct second component towards χ^1 Ori, which is closer to the downwind He° vector, suggests the angular scale of the BC does not have significant column densities in the downwind He° direction. If instead the local cloud is filamentary, with the bulk LSR CLIC flow perpendicular to an ISMF in an expanding filamentary shell, then both χ^1 Ori and α Aur are still relatively close to the LSR CLIC downwind direction ($\theta_{\rm CLIC}$= 146°, 171°), so these timescales may still be roughly valid.

The alternative of filamentary structures seem appropriate, given the widespread appearance of filamentary clouds when magnetic fields are present, and given the configuration favored by the perpendicular ISMF direction and CLIC bulk LSR motion of an expanding superbubble shell containing magnetically aligned filaments. For a filamentary structure, α CMa and ϵ CMa are nearly aligned with the filament since $\theta_{\rm CLIC}$=86°–106°, and the α CMa sightline is 16° from the ISMF direction. The case where α CMa is sighted along the cloud surface was considered by Frisch (1994), who concluded that the Sun could have entered the CISM gas anytime within the past 2,000-8,000 years, or sooner given the uncertainties. If the surface is corrugated, or curved, then the sightlines to one of the stars might traverse conductive interface regions on the cloud. The C^{+++} detected towards ϵ CMa suggests the presence of an interface.

For the sake of comparisons with the geologic radio isotope record, and because the downwind gas must be either clumpy or filamentary, we adopt several time intervals as possible candidates for a solar transition between interstellar clouds. These transitions are: (1) Sometime within the past 8,000 years, as indicated by the α CMa sightline together with an assumed filamentary cloud structure; (2) Sometime within $10,000 - 32,000$ years ago. Two clouds are seen towards α CMa and α CMi, 3.5 pc, and the second cloud should be more ionized than the CISM since it is unshielded from ϵ CMa, the primary source of local H-ionization. This suggests that there was more ionized and clumpy ISM around the Sun before we entered the CISM gas, or perhaps a cloud interface. We estimate 30% of the α CMi sightline is filled with neutral ISM for $n(H^\circ)$=0.2 cm^{-3}. Strictly speaking, going by velocities only, the Sun could have encountered this ISM anytime within the past $\sim 175,000$ years. However the clumpiness of the local ISM, and the apparent deceleration evident in the CLIC velocities, suggest that the clumps of gas that form the CLIC have a cohesive origin and are close to each other. The obvious uncertainties in these time scales include the cloud shape and unknown volume densities. If cloud densities are lower than the CISM value of $n(H^\circ)$=0.2 cm^{-3}assumed here, they are more extended than listed in Table 1; if densities are larger, clouds will be less extended.

3 The Heliosphere for Different Interstellar Environments

The heliosphere results from a balance between solar wind and interstellar pressure. This balance sets the size of the heliosphere and determines the particle distributions and magnetic field configurations throughout, which in turn determine how galactic cosmic rays are being modulated during their passage through the heliosphere on their way to Earth.

The inner boundary conditions of the heliosphere consist of the solar wind, imprinted with the 22 year magnetic activity cycle of the Sun, as a "point source" inflow. The time variability of the solar wind affects the large-scale heliosphere, including the heliosheath regions. The distance of the termination shock in the nose direction varies by about 10 AU with the solar cycle phase, and is closer during solar wind minima when ram pressures are lower (Zank and Müller 2003). The reversals of the solar magnetic polarity every ~ 11 years between successive solar minima propagate to the inner heliosheath regions, and create bands of magnetic polarity that are swept around the flanks of the heliosphere with the subsonic solar wind (e.g., Pogorelov *et al.* 2009). The outer boundary conditions of the heliosphere are dominated by the total pressure of the surrounding cloud, including magnetic pressure, the ram pressure of excluded ions, and a large fraction of the ram pressure of the neutrals which participate through charge-exchange with ions outside the heliopause (the pressure interior of the heliopause is modified by charge exchange as well).

Configurations of the global heliosphere have been modeled for a range of surrounding interstellar cloud properties. In one study (Müller *et al.* 2008), the parameter space around the current interstellar cloud is sampled to establish empirical relations for locations of heliopause, termination shock, and bow shock as a function of interstellar boundary values. This study confirms the overall connection of the size of the heliosphere with the pressure balance argument. The interstellar ionization ratio weakly influences the downstream termination shock distance as well as the typical termination shock strength. In relative terms, the termination shock shape does not change in this particular region of parameter space. Müller *et al.* (2006) explore a wider range of possible interstellar environments, including cold dense clouds, hot tenuous, completely ionized clouds like what was assumed for the Local Bubble, and systems on galactic paths that result in fast relative Sun-ISM velocities. In particular the relative velocity has a decisive influence on how much interstellar neutral material reaches the inner heliosphere (filtration); the larger the relative velocity, the less filtration is occurring. If the Sun encounters a completely ionized ISM (Local Bubble), GCR particle fluxes at Earth are lower than currently. With neutrals absent, none of the pressure balance modifications take place, and secondary particles like anomalous cosmic rays (ACR) do not exist. Lastly, if the heliosphere is embedded in a dense cloud, the heliosphere is small in size, and particle fluxes at Earth rise substantially. Depending on the interstellar ram pressure, the heliosphere can easily get small enough for the Earth orbit being partly in the inner heliosheath region.

Yeghikyan and Fahr (2006) consider the passage of very dense molecular clouds over the heliosphere. The resulting heliospheres are very small, so that the orbit of Earth takes it through regions of interstellar gas outside the heliopause. The expected neutral fluxes at Earth are so high that changes for the ozone layer and other climate-related effects are to be expected. Similarly, when a supernova shock front washes over the heliosphere (Müller *et al.* 2009), the heliosphere can be equally small (Figure 2a), with direct access of supernova material to the Earth atmosphere. In both cases of

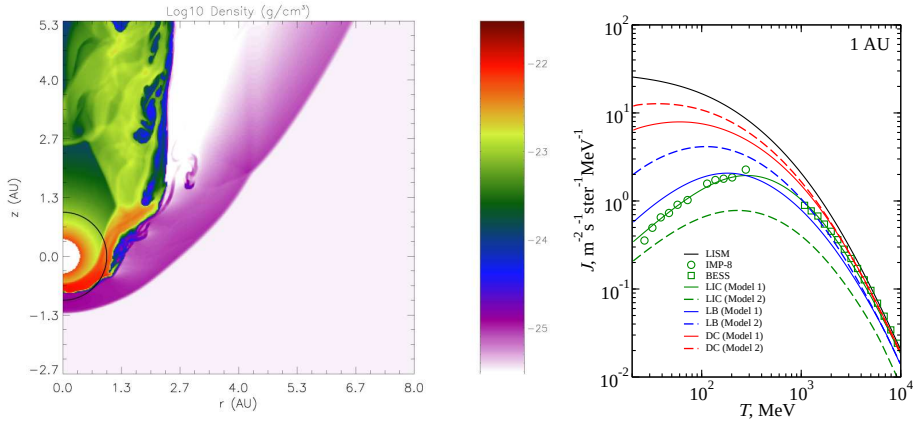

Fig. 2 *Left.* Snapshot of the heliospheric density during a supernova shock arrival, for previously CISM-like ambient conditions (the SNR velocity is 12,000 km s^{-1}). Earth's orbit is indicated as a circle (neglecting inclination effects). Earth is directly exposed to SNR material for part of the year. *Right.* Spectra of galactic cosmic rays at 1 AU for three different interstellar clouds surrounding the heliosphere: LIC stands for the contemporary CISM; LB is the Local Bubble interior modeled as a 1.2×10^6 K fully ionized plasma with density 0.005 cm^{-3}; and DC is a dense cloud with density 10 cm^{-3}, temperature 200 K, and relative velocity of 25 km s^{-1}. The figures are from Müller *et al.* (2009) and Müller *et al.* (2006), respectively.

extremely small heliospheres, the access of GCR to Earth is greatly enhanced. In a calculation by Florinski *et al.* (2003), where a cold dense cloud results in a moderate size heliosphere of 23 AU, a two-fold flux of GCR, and a ten-fold flux of ACR is reported. Figure 2b illustrates this with calculated spectra for the Local Bubble case and for a dense cloud case, comparing them to the GCR fluxes of the contemporary heliosphere.

4 Comparing past cloud transitions with the terrestrial radioisotope record

The radioisotopes ^{10}Be, ^{36}Cl, and ^{14}C are created by GCR spallation in the terrestrial atmosphere, and precipitate to Earth and form geological records that serve as a tracer of cosmic ray fluxes interacting with the Earth's magnetic field (e.g. see articles by McCracken and Beer in this volume). The well known anticorrelation between GCR fluxes arriving at Earth and the solar activity cycle (see articles by Leske and Mewaldt in this volume) suggests that interstellar-driven variations in the heliosphere configuration also may have an effect on the GCR flux impinging on the Earth's surface. Section 3 discusses the response of the heliosphere, and examples of substantial variations in GCR modulation for some ISM-heliosphere interactions. In this section, we search for evidence of such an effect.

Methods for reconstructing the paleomagnetic field of the Earth rely on comparing GCR-generated radio isotopes ^{10}Be, ^{36}Cl, and ^{14}C with remanence magnetic field measurements (Muscheler *et al.* 2005, M05). Several anomalies are found in these comparisons, where the different methods for reconstructing the terrestrial magnetic dipole

components do not agree. These puzzling differences provide the opportunity for explanations that rely on interstellar perturbations of the heliosphere, and the resulting modulation of the 1 AU cosmic ray flux. Previous efforts to explain ^{10}Be anomalies include a modulation by a diminished heliosphere due to a passing supernova shock (Sonett *et al.* 1987, and see Fig. 2), unconfirmed results that link peaks in the ^{10}Be ice core records with the passage of the Sun through magnetic flux tubes in the ISM (Frisch 1997), and the careful study of the effect of the Maunder Minimum on ^{10}Be in ice cores (McCracken 2004). Although high GCR fluxes are linked to climate cooling (e.g., Kirkby and Carslaw 2006), such processes are not discussed here.

The unexplained discrepancies in the paleomagnetic record result from discrepant reconstructions of the paleomagnetic field from remanence measurements, and from tracking the radio isotope fluxes in ice core (^{10}Be, ^{36}Cl) and tree ring (^{14}C) records. The ones we discuss here include: (1) The discrepancy in the timing of the maximum magnetic field dipole strengths (the "virtual axis dipole moment", VADM) during the Holocene traced by the ^{10}Be versus ^{14}C records (Fig. 6 in M05). (2) The 18,000–34,000 years ago record where both ^{10}Be and ^{36}Cl VADM reconstructions differ from the remanence records, and the ^{14}C data are less understood.

(1) The VADM paleomagnetic field reconstructed from ^{10}Be records peaks at 2,000 years BP, which is one millennium later than the peak determined from ^{14}C at 3,000 years BP (Fig. 6 in M05). The ^{10}Be and archeomagnetic field determinations agree generally, so that the discrepancy is postulated to be due to the carbon cycle (M05). Since increases in VADM strengths indicate reduced radio isotope fluxes, the reduction in the ^{14}C fluxes occurred about a millennium before the reduction in the ^{10}Be fluxes in the holocene. This time interval is within the uncertainties of the solar entry into the LIC, as determined from the α CMa sightline and assumed filamentary structure. We postulate that prior to entering the CISM, the Sun traversed an ionized cloud interface region that did not contain any interstellar neutrals, and which generated higher ram pressures because of larger velocities from outflows (Fig. 2 in SF08). This would have reduced the GCR modulation region, but also removed entirely the anomalous cosmic rays (ACRs) that form from accelerated interstellar neutrals. We speculate that the ^{14}C concentrations, but not ^{10}Be or ^{36}Cl, are enriched by lower energy ACRs, because the long dwell times of ^{14}C in the troposphere allows the ^{14}C concentration to be enriched with ACRs trapped in the radiation belts of the Earth (Mewaldt *et al.* 1998). As a consequence, the ^{14}C flux would immediately see two effects upon entering an ionized interface, one due to ionization and the disappearance of ACRs, which leads to a decrease in ^{14}C according to our hypothesis, and the other which works in concert with ^{10}Be modulation and shows an increased flux because of the smaller heliosphere. As the Sun enters the main part of the cloud, which is $\sim 23\%$ ionized (SF08), the balance between the synchronization of the ^{10}Be, ^{36}Cl, and ^{14}C formation was restored along with neutrals and the ACRs. The general implication is that when ^{10}Be, ^{36}Cl, and ^{14}C fluxes are synchronized in the paleomagnetic record, this would sample an interval when the ISM surrounding the heliosphere contains neutrals. However because ^{14}C would be further enriched by ACRs trapped in the radiation belts, the absence of interstellar neutrals would decrease ^{14}C concentrations relative to ^{10}Be and ^{36}Cl.

(2) During the period 18,000–34,000 years ago, both the ^{10}Be and ^{36}Cl VADM reconstructions deviate from the remanence archeomagnetic records. The increased VADM reconstructed from ^{10}Be and ^{36}Cl suggests reduced fluxes below that explained by the archeomagnetic record, or extra heliosphere modulation of GCRs. M05 suggested that possible changes in levels of solar magnetic activity may be responsible for this

difference. We speculate that this interval instead corresponds to an encounter between the Sun and slower clumpy ISM beyond the CISM in the downwind direction that forms the second clouds observed towards α CMa and α CMi, both within 3.5 pc. Cloud velocities alone affect the GCR modulation because the heliosphere dimensions increase as the ram pressure of the ISM decreases. The decreased ^{10}Be and ^{36}Cl fluxes in this interval would then suggest a larger heliosphere modulation region, that still contains a solar wind mass-loaded with interstellar particles. Cloud-Sun relative velocities of 26 km s^{-1} today, versus 21–22 km s^{-1} for χ^1 Ori and α Aur, and 14 km s^{-1} for the BC towards α CMa (Table 1), suggest that cloud ram pressure could have been a factor of $\sim 2-3$ lower in the past than today, giving a larger heliosphere and larger GCR modulation region that are consistent with the decreased fluxes found by M05.

Additional discrepancies, about 48,000 and 58,000 years ago, are seen between the radio isotope paleomagnetic and remanence paleomagnetic records. These timescales are well within uncertainties on the entry times of the Sun into nearby interstellar clouds (Table 1), however there is little detailed interstellar information on which to base a comparison.

5 Future: Improving Comparisons between Local ISM Structure and Paleomagnetic Records

The comparisons between the structure and kinematics of interstellar clouds near the Sun, and the paleomagnetic records deduced from radio isotopes such as ^{10}Be, ^{36}Cl, and ^{14}C, are based on scanty knowledge of details of the three-dimensional spatial distribution and configuration of nearby interstellar clouds. In addition, the flux of galactic and anomalous cosmic rays at the Earth has only been calculated for a limited number of heliosphere configurations (e.g. Florinski this volume, Florinski and Zank 2006)). Given the uncertainties, the attenuation of GCRs and ACRs by an ISM-modulated heliosphere appears to be capable of accounting for several unexplained excursions in the geomagnetic record. More study of the roles of anomalous cosmic rays versus higher GCRs as source populations of the radio isotopes will be of interest, since differences between the ^{14}C, ^{10}Be, ^{36}Cl records are mandated if ACRs are a factor in ^{14}C production rates. Only more data will reveal whether these interpretations are accurate.

Acknowledgements PCF thanks the International Space Sciences Institute in Bern, Switzerland, for hosting a stimulating meeting on the relation between cosmic ray fluxes and the terrestrial radio isotope record. This research has been supported in part by NASA grants NNX09AH50G and NNX08AJ33G to the University of Chicago, and by the IBEX mission as a part of NASA's Explorer Program. PCF would like to thank Ken McCracken and Jurg Beer for helpful discussions.

References

Allen, C. W. (1973). *Astrophysical Quantities*. AthlonePress.

Balsara, D., Benjamin, R. A., and Cox, D. P. (2001). The Evolution of Adiabatic Supernova Remnants in a Turbulent, Magnetized Medium. *Astrophys. J.*, **563**, 800–805.

Bohlin, R. C., Savage, B. D., and Drake, J. F. (1978). A survey of interstellar H I from L-alpha absorption measurements. . *Astrophys. J.*, **224**, 132–142.

Crawford, I. A. (1992). High-resolution observations of the interstellar 3302-wavelength Na I doublet and a discussion of the resulting Na I/Ca II ratios. *MNRAS*, **259**, 47–62.

de Geus, E. J. (1992). Interactions of stars and interstellar matter in Scorpio Centaurus. *Astron. Astrophys.*, **262**, 258–270.

Florinski, V. and Zank, G. P. (2006). The Galactic Cosmic Ray Intensity in the Heliosphere in Response to Variable Interstellar Environments. In *Solar Journey: The Significance of Our Galactic Environment for the Heliosphere and Earth*, pages 281–316 . Springer.

Florinski, V., Zank, G. P., and Axford, W. I. (2003). The Solar System in a dense interstellar cloud: Implications for cosmic-ray fluxes at Earth and ^{10}Be records. *Geophys. Res. Lett.*, **30**, 5–1.

Frisch, P. C. (1981). The nearby interstellar medium. *Nature*, **293**, 377–379.

Frisch, P. C. (1994). Morphology and ionization of the interstellar cloud surrounding the solar system. *Science*, **265**, 1423.

Frisch, P. C. (1997). Journey of the Sun, astro-ph/9705231. *arXiv*.

Frisch, P. C. (2010). The S1 Shell and Interstellar Magnetic Field and Gas Near the Heliosphere. *Astrophys. J.*, **714**, 1679–1688.

Frisch, P. C. and McComas, D. J. (2010). The Interstellar Boundary Explorer (IBEX): Tracing the Interaction between the Heliosphere and Surrounding Interstellar Material with Energetic Neutral Atoms. *Space Sci. Rev., submitted*, **00**, 0–0.

Frisch, P. C. and Slavin, J. D. (2006). Short Term Variations in the Galactic Environment of the Sun, in *Solar Journey: The Significance of Our Galactic Environment for the Heliosphere and Earth*, Ed. P. C. Frisch. Springer.

Frisch, P. C., Dorschner, J. M., Geiss, J., Greenberg, J. M., Grün, E., Landgraf, M., Hoppe, P., Jones, A. P., Krätschmer, W., Linde, T. J., Morfill, G. E., Reach, W., Slavin, J. D., Svestka, J., Witt, A. N., and Zank, G. P. (1999). Dust in the Local Interstellar Wind. *Astrophys. J.*, **525**, 492–516.

Frisch, P. C., Bzowski, M., Grün, E., Izmodenov, V., Krüger, H., Linsky, J. L., McComas, D. J., Möbius, E., Redfield, S., Schwadron, N., Shelton, R. R., Slavin, J. D., and Wood, B. E. (2009). The Galactic Environment of the Sun: Interstellar Material Inside and Outside of the Heliosphere. *Space Sci. Rev.*, pages 28–+.

Frisch, P. C., Andersson, B.-G., Berdyugin, A., Funsten, H. O., McComas, D. J., Piirola, V., Schwadron, N. A., Slavin, J. D., and Wiktorowicz, S. J. (2010). Comparisons of the Interstellar Magnetic Field Direction sobtained from the IBEX Ribbon and Interstellar Polarizations. *ApJ, in press, Nov. 10*, **00**, 0–0.

Gosling, J. T. (1964). A Study of the Relationship between Absorption-Time Profiles of Polar-Cap-Absorption Events and Forbush Decreases of Cosmic Ray Intensity. *J. Geophys. Res.*, **69**, 1233–1238.

Hebrard, G., Mallouris, C., Ferlet, R., Koester, D., Lemoine, M., Vidal-Madjar, A., and York, D. (1999). Ultraviolet observations of Sirius A and Sirius B with HST-GHRS. An interstellar cloud with a possible low deuterium abundance. *Astron. Astrophys.*, **350**, 643–658.

Heiles, C. (1998). Whence the Local Bubble, Gum, Orion? GSH 238+00+09, A nearby major superbubble toward Galactic longitude 238 degrees. *Astrophys. J.*, **498**, 689–703.

Holzer, T. E. (1989). Interaction between the solar wind and the interstellar medium. *ARA&A*, **27**, 199–234.

Kirkby, J. and Carslaw, K. S. (2006). Variations of Galactic Cosmic Rays and the Earth's Climate. In *Solar Journey: The Significance of Our Galactic Environment for the Heliosphere and Earth*, page 000. Springer, Ed. P. C. Frisch.

Koutroumpa, D., Lallement, R., Kharchenko, V., and Dalgarno, A. (2009). The Solar Wind Charge-eXchange Contribution to the Local Soft X-ray Background. Model to Data Comparison in the 0.1-1.0 keV Band. *Space Science Reviews*, **143**, 217–230.

Müller, H.-R. and Zank, G. P. (2004). Heliospheric filtration of interstellar heavy atoms: Sensitivity to hydrogen background. *J. Geophys. Res.*, **109, A07104**, 7104–7116.

McCammon, D., Burrows, D. N., Sanders, W. T., and Kraushaar, W. L. (1983). The soft X-ray diffuse background. *Astrophys. J.*, **269**, 107–135.

McCracken, K. G. (2004). Geomagnetic and atmospheric effects upon the cosmogenic Be10 observed in polar ice. *J. Geophys. Res.*, **109**, 4101–+.

Mewaldt, R. A., Cummings, A. C., and Stone, E. C. (1998). Anomalous Cosmic Ray: Interstellar Interlopers in the Heliosphere and Magnetosphere. In S. T. Suess & B. T. Tsurutani, editor, *From the Sun, Auroras, Magnetic Storms, Solar Flares, Cosmic Rays*, pages 133–+.

Meyer, D. M., Lauroesch, J. T., Heiles, C., Peek, J. E. G., and Engelhorn, K. (2006). A Cold Nearby Cloud inside the Local Bubble. *Astrophys. J. Lett.*, **650**, L67–L70.

Möbius, E., Bzowski, M., Chalov, S., Fahr, H., Gloeckler, G., Izmodenov, V., Kallenbach, R., Lallement, R., McMullin, D., Noda, H., Oka, M., Pauluhn, A., Raymond, J., Ruciński, D., Skoug, R., Terasawa, T., Thompson, W., Vallerga, J., von Steiger, R., and Witte, M. (2004). Synopsis of the interstellar He parameters from combined neutral gas, pickup ion and UV scattering observations and related consequences. *Astron. Astrophys.*, **426**, 897–907.

Müller, H., Woodman, L. M., and Zank, G. P. (2008). Heliospheric termination shock strength from a multi-fluid model. In G. Li, Q. Hu, O. Verkhoglyadova, G. P. Zank, R. P. Lin, & J. Luhmann , editor, *American Institute of Physics Conference Series*, volume 1039 of *American Institute of Physics Conference Series*, pages 384–389.

Müller, H., Frisch, P. C., Fields, B. D., and Zank, G. P. (2009). The Heliosphere in Time. *Space Sci. Rev.*, **143**, 415–425.

Müller, H.-R., Frisch, P. C., Florinski, V., and Zank, G. P. (2006). Heliospheric response to different possible interstellar environments. *Astrophys. J.*, **647**, 1491–1505.

Muscheler, R., Beer, J., Kubik, P. W., and Synal, H. (2005). Geomagnetic field intensity during the last 60,000 years based on Be10 and Cl36 from the Summit ice cores and C14. *Quaternary Science Reviews*, **24**, 1849–1860.

Perryman, M. A. C. (1997). The HIPPARCOS Catalogue. *Astron. Astrophys.*, **323**, L49–L52.

Pogorelov, N. V., Borovikov, S. N., Zank, G. P., and Ogino, T. (2009). Three-Dimensional Features of the Outer Heliosphere Due to Coupling Between the Interstellar and Interplanetary Magnetic Fields. III. The Effects of Solar Rotation and Activity Cycle. *Astrophys. J.*, **696**, 1478–1490.

Redfield, S. and Linsky, J. L. (2002). The Structure of the Local Interstellar Medium. I. High-Resolution Observations of Fe II, Mg II, and Ca II toward Stars within 100 Parsecs. *Astrophys. J. Suppl.*, **139**, 439–465.

Redfield, S. and Linsky, J. L. (2008). The Structure of the Local Interstellar Medium. IV. Dynamics, Morphology, Physical Properties, and Implications of Cloud-Cloud Interactions. *Astrophys. J.*, **673**, 283–314.

Salvati, M. (2010). The local Galactic magnetic field in the direction of Geminga. *Astron. Astrophys.*, **513**, A28+.

Schönrich, R., Binney, J., and Dehnen, W. (2010). Local kinematics and the local standard of rest. *MNRAS*, **403**, 1829–1833.

Slavin, J. D. and Frisch, P. C. (2008). The boundary conditions of the heliosphere: photoionization models constrained by interstellar and in situ data. *Astron. Astrophys.*, **491**, 53–68.

Sonett, C. P., Morfill, G. E., and Jokipii, J. R. (1987). Interstellar Shock Waves and 10Be from Ice Cores. *Nature*, **330**, 458.

Stanimirović, S. (2009). Exotic Clouds in the Local Interstellar Medium. *Space Sci. Rev.*, **143**, 291–301.

Stone, J. M. and Zweibel, E. G. (2010). Ambipolar Diffusion-Mediated Thermal Fronts in the Neutral ISM. *ArXiv e-prints*.

Wolleben, M. (2007). A New Model for the Loop I (North Polar Spur) Region. *Astrophys. J.*, **664**, 349–356.

Wood, B. E., Linsky, J. L., and Zank, G. P. (2000). Heliospheric, astrospheric, and interstellar ly-alpha; absorption toward 36 Ophiuchi. *Astrophys. J.*, **537**, 304–311.

Wood, B. E., Redfield, S., Linsky, J. L., Müller, H.-R., and Zank, G. P. (2005). Stellar Lyα Emission Lines in the Hubble Space Telescope Archive: Intrinsic Line Fluxes and Absorption from the Heliosphere and Astrospheres. *Astrophys. J. Suppl.*, **159**, 118–140.

Yeghikyan, A. and Fahr, H. (2006). Accretion of interstellar material into the heliosphere and onto Earth, in *Solar Journey: The Significance of Our Galactic Environment for the Heliosphere and Earth*, Ed. P. C. Frisch. Springer.

Zank, G. P. and Müller, H.-R. (2003). The dynamical heliosphere. *J. Geophys. Res.*, **108**.